OVERCOMING ABCG2-MEDIATED DRUG RESISTANCE WITH IMIDAZO-[1,2-b]-PYRIDAZINE BASED PIM1 KINASE INHIBITORS

Richard A.J. Darby[1,2], Amanda Unsworth[1], Simon Brooks[1], Stefan Knapp[2], Ian D Kerr[3] and *Richard Callaghan[1,4]

1 Nuffield Department of Clinical Laboratory Sciences, John Radcliffe Hospital, The University of Oxford, Headington, U.K.

2 Structural Genomics Consortium and Target Discovery Institute The University of Oxford, Old Road Campus, NDM Research Building, Oxford OX3 7FZ Oxford, U.K.

3 School of Biomedical Sciences, University of Nottingham, Queen's Medical Centre, Nottingham, NG7 2UH.UK.

4 Division of Biomedical Science & Biochemistry, Research School of Biology, The Australian National University Canberra, ACT 0200, Australia

Running Title: Inhibition of ABCG2 by targeting Pim-1 kinase

* To whom all correspondence should be addressed

E-mail: richard.callaghan@anu.edu.au

Tel: +61 2 6125 0824

ABSTRACT

Multidrug efflux pumps such as ABCG2 confer drug resistance to a number of cancer types, leading to poor prognosis and outcome. To date the strategy of directly inhibiting multidrug efflux pumps in order to overcome drug resistance in cancer has been unsuccessful. An alternative strategy is to target proteins involved in the regulation of multidrug efflux pump activity or expression. Pim-1 Kinase has been demonstrated to phosphorylate ABCG2, promote its oligomerisation and contribute to its ability to confer drug resistance. In the present manuscript, imidazo-pyridazine based inhibitors of Pim-1 were examined for their ability to overcome ABCG2 mediated drug resistance. We show that two Pim-1 inhibitors of this inhibitor class increased potency of flavopiridol, mitoxantrone, topotecan and doxorubicin specifically in ABCG2 expressing cells. This effect was associated with an increase in the cellular accumulation of [^{3}H]-mitoxantrone, suggesting a impairment of the transporter. However, prolonged pre-incubation with the studied Pim-1 inhibitors greatly enhanced the effect on mitoxantrone accumulation. The inhibitors caused a significant time-dependent reduction in the expression of ABCG2 in the resistant cells, an effect that would improve drug efficacy. Consequently, it appears that the Pim-1 inhibitors display a dual mode effect on ABCG2 expressing cancer cells providing a powerful new strategy in over-coming drug resistance by targeting proteins that regulate expression of efflux pumps.

KEYWORDS:

Multi-drug resistance, BCRP, ABCG2, Pim-1 kinase, Cancer chemotherapy

1. INTRODUCTION

Chemotherapy remains a vital treatment strategy in cancer and unfortunately, the multidrug resistant phenotype continues to confound its efficacy. Multidrug resistance comprises numerous cellular processes that are either inherent to the tissue or acquired during chemotherapy. The plasma membrane is at the front-line of resistance and utilises a triad of drug efflux pumps from the ATP Binding Cassette (ABC) family. The three pumps have distinct pharmacological profiles and distinct expression patterns in cancer. The focus of this investigation is ABCG2, which is known to confer resistance to flavopiridol, mitoxantrone, methotrexate and topotecan [1, 2]. The protein is expressed in cultured cell lines of fibrosarcoma, myeloma, ovarian and breast cancer. Human cancers known to express the protein include digestive tract, lung and endometrial adenocarcinomas, soft-tissue sarcomas and haematological malignancies [2-6]. At the clinical level, there are no effective strategies to overcome the resistant phenotype produced by ABCG2; although a number of compounds inhibit its activity *in vitro*. Developing strategies to overcome the action of ABCG2 are important, particularly given its wide expression profile in cancers and the number of cytotoxic drugs affected by its influence.

A homodimeric assembly of ABCG2 is required to generate a fully functional drug transport protein. The precise oligomeric status remains contentious with evidence from co-immunoprecipitation [7] and low resolution cryo-EM studies indicating the presence of higher order oligomers [8].The protein is a member of the G-sub-family and comprises an amino-terminal nucleotide binding domain (NBD) and a transmembrane domain (TMD) containing six helices [1]. This “reverse” topological arrangement is distinct from other sub-groups of the ABC family. The protein is glycosylated on the asparagine at position 596 [9], which is located in the extracellular loop between TM helices 5 and 6. This loop also contains a disulfide bond between cysteine residues at positions 592 and 608 [10]. The precise roles of glycosylation and disulfide bond formation in ABCG2 function remain unresolved, but they are crucial to the folding and stability of the protein. The region at the interface between homo-dimeric units remains to be elucidated, although a GXXXG motif between positions 406-410 has been implicated [11].

ABCG2 has numerous consensus sites for phosphorylation, although there is little information on the state of its phosphorylation in cells [1, 12, 13]. However, phosphorylation of ABCG2 has been suggested to be a prerequisite for its expression at the plasma membrane with a report showing that activation of protein kinase B (AKT) results in an

increase in the amount of ABCG2 at the plasma membrane; whilst inactivation of ATK results in internal retention of ABCG2 [12]. Moreover, the interaction has a functional consequence since it has been shown in haematopoietic stem cells that the efflux of the ABCG2 substrate Hoechst 33342 was positively correlated with the activity of ATK [14].

Activated AKT has also been shown to bind to the prolactin response element found on the *pim-1* promoter [15]. Pim1 kinase is a serine/threonine kinase encoded by a proto-oncogene known to be expressed in several cancers [16]. Two isoforms of the kinase are known to be produced by alternative translation start sites yielding a 33 and 44 kDa protein. The 44 kDa kinase is found complexed, whilst the 33 kDa isoform is monomeric [17]. Whilst the 33 kDa kinase regulates the cell cycle and transcription by phosphorylating numerous participants in these processes, including cdc25A, HP1 and p100 [18-21], the 44kDa kinase has been shown to interact with ABCG2 [13]. It potentially phosphorylates a Threonine residue at position 362, which is thought to be vital for the dimerization and/or multimerisation of ABCG2. This induces a conformational change to promote the formation of an inter-molecular disulphide bond with Cys374, resulting in active ABCG2 at the plasma membrane [13]. The Thr362 residue in ABCG2 is found in a Pim1 compatible recognition sequence: $(Lys)_3$-Ile-**Thr-**Val [22]. In a taxane-resistant prostate cancer cell line over-expressing P-gp, treatment with SGI-1776 (a novel inhibitor of Pim1) re-sensitised the cell line to paclitaxel suggesting a potential role for Pim1 kinase in multidrug-resistance [23].

Compounds based on an imidazo[1,2-b]pyridazine scaffold are ATP competitive inhibitors with good target selectivity that have been found to inhibit Pim1 kinase at nanomolar concentrations in vitro [24]. This class of compounds also display selectivity for the Pim-1 kinase domain over the Pim-2 isoform. K00135 and K00486 (Figure 1), were identified as the best compounds of this series to bind to Pim-1 with a high affinity and inhibit its activity [25]. The present study investigated the effects of the Pim-1 kinase inhibitors K00135 and K00486 on ABCG2 mediated drug resistance in the $MCF7^{FLV1000}$ cell line. The data suggest that the inhibitors are able to overcome drug resistance by a dual mechanism involving direct inhibition of ABCG2 and by altering its expression.

2. MATERIALS & METHODS

2.1 Reagents

The imidazo-[1,2-b]-pyridazine based Pim1 kinase inhibitors were synthesised in the Knapp Laboratory and stored at a concentration of 50mM in DMSO. The ABCG2 specific inhibitor fumitremorgin C (FTC), doxorubicin, topotecan and mitoxantrone were purchased from Sigma Aldrich and prepared as 50mM aliquots in DMSO. Mitoxantrone (Tocris) was prepared at 50mM in DMSO and flavopiridol (Biomol International) was prepared at 10mM in DMSO. All compounds were stored at -20˚C. [^{3}H]-Mitoxantrone (148 GBq/mmol) was purchased from Moravek Biochemicals (Brea, USA). The anti-ABCG2 (BXP-21) and the anti-Pim antibody (12H8) were purchased from Santa-Cruz Biotechnology and the goat anti-mouse horseradish peroxidase conjugated antibody from DAKO. The ECL Prime chemi-luminescence detection kit was purchased from GE. All plasticware was purchased from either Fisher Scientific UK or Greiner Bio-One.

2.2 Cell lines

A549 (lung), DLD-1 (colorectal), H226 (lung), HT-29 (colorectal), LnCaP (prostate), PC3 (prostate), MCF7 (breast) and the ABCG2-overexpressing MCF7^{FLV1000} cell lines were cultured in RPMI 1640 medium (Invitrogen Life Technologies) supplemented with 10 % foetal calf serum and 1% penicillin/streptomycin (Lonza). Flavopiridol (500nM) was added to the medium of the MCF7^{FLV1000} cell line every 4th sub-culture to maintain selection pressure for ABCG2 expression. Cells were maintained for a further passage before use. The JURKAT and K562 leukaemic cell lines were grown under similar conditions but as suspension cultures.

2.3 Cytotoxicity Assays

Cells were seeded in flat-bottomed 96-well plates at a density of 2,500 cells per well and allowed to attach to the surface for 24 hours at 37 ºC, 5 % CO_2. The effects of single drug treatment on the viability of the cell lines were evaluated after incubation for 5 days with various concentrations of Pim kinase inhibitors (10^{-8}-10^{-4}M) or chemotherapeutic agents (10^{-12}-10^{-4}M).

For combination drug treatment, MCF7 and MCF7^{FLV1000} cell lines were incubated with chemotherapeutic agents (10^{-12}-10^{-4}M) in the absence or presence of FTC (0.3μM), K00135 (0.1 or 0.3μM), K00486 (0.3 or 1.0μM), or an equivalent volume of DMSO as a positive

control and allowed to incubate for 5 days at 37ºC, 5% CO_2. Cells were subsequently fixed in 10 % trichloroacetic acid for 30 minutes at 4ºC. The plates were then washed with 5 rounds of water and stained with 0.075% (w/v) sulforhodamine B (SRB) for 15 minutes at room temperature. Excess SRB was removed from the plates with four washes of 1% (v/v) acetic acid and the SRB stained viable cells solubilised with 10mM Trizma pH10.5. Absorbance was detected on a SpectraMax Plus 384 (Molecular Devices) at 540 nm using SoftMax®Pro data acquisition and analysis software. For the non-adherent leukaemia cells the MTS assay was used to measure cell density and viability as described [26].

Data from either assay was subsequently analysed and graphically depicted using GraphPad Prism software, using 1-way ANOVA analysis. Drug toxicity was quantified by non-linear regression of the general dose-response equation:

$$F = F_{min} + \frac{F_{max} - F_{min}}{1 + 10^{(log_{10}(IC_{50}) - [D])}}$$

Where F is the viable cell number, F_{max} and F_{min} are the maximum and minimum cell number respectively, IC_{50} is the concentration causing 50% cell death and $[D]$ is the logarithm of drug concentration. At least four independent experiments were performed and relative resistance values were established by dividing the IC_{50} value of the $MCF7^{FLV1000}$ cell line for each drug by the IC_{50} value of the MCF7 cell line.

2.4 Cellular accumulation of [^{3}H]-Mitoxantrone

ABCG2 mediated transport was assessed by the steady-state accumulation of [^{3}H]-mitoxantrone. 50,000 cells well^{-1} were seeded in sterile 24-well plates and incubated at 37ºC, 5% CO_2 overnight. Pim1-kinase inhibitors or FTC were added to the wells and allowed to incubate for various times as specifically indicated in the results. The medium was subsequently discarded from the plate and replaced with 0.5 ml of drug transport buffer (107mM NaCl, 10mM Tris.HCl pH7.4, 26mM $NaHCO_3$, 5.3mM KCl, 1.9mM $CaCl_2$, 1mM $MgCl_2$, 7mM glucose) containing a total mitoxantrone concentration of 1μM, which contained 40nM of the tracer [^{3}H]-mitoxantrone. FTC or Pim-kinase inhibitor were also added to the transport buffer with radioligand where required. The plate was incubated as above for a period of 3 hours before discarding the buffer and washing the wells 3 times with 0.5 ml of ice-cold PBS. The cells were lysed with 0.5 ml 0.1 M NaOH and the amount of mitoxantrone

determined by liquid scintillation with 3.5 ml of ReadyProtein scintillation fluid for 5 minutes. The radioactive decay was converted to nmoles of mitoxantrone accumulated per mg of cell protein using the specific activity of the radioligand.

2.5 Western immuno-blot analysis

Cells were washed with PBS and lysed with 1% (w/v) SDS and subsequently sheared with a fine gauge needle. Protein concentration was determined using the detergent compatible DC BioRad assay using BSA as a standard. Samples of lysate (5-20μg as indicated in figure legends) were subjected to SDS-PAGE using 10% (w/v) gels and then transferred to nitrocellulose. The nitrocellulose was blocked for 1 hour with 5% (w/v) non-fat dried milk in PBS containing 0.1% (v/v) Tween 20. The antibodies were diluted according to the manufacturers' protocols in 5% (w/v) non-fat dried milk in PBS containing 0.1% (v/v) Tween 20 and incubated with the nitrocellulose overnight. Following washing in PBS containing 0.1% (v/v) Tween 20, the nitrocellulose was incubated with goat anti-mouse HRP secondary antibody for 1 hour. The immuno-blots were developed using ECL Prime chemi-luminescence according to the manufacturer's instructions, exposed to Hyperfilm ECL and analysed by densitometry using ImageJ software.

3. RESULTS

Imidazo-[1,2-b]-pyridazine inhibitors have previously been demonstrated to interact with the nucleotide binding site of Pim-1. The two inhibitors (K00135 and K00486) used in this investigation (Figure 1) were generated from structure-activity relationships with Pim1 and they represent two of the most potent available Pim1 inhibitors.

3.1 Growth inhibitory effects of Pim1 inhibitors in cultured cancer cell lines

Initial studies with Pim kinases were confined to leukaemia and lymphoma cells although over-expression in biopsy samples had been subsequently confirmed in solid tumours. Both Pim-1 inhibitors produced growth arrest in the K562 and JURKAT leukaemia cell lines (Table 1). The potencies did not differ significantly between K00135 and K00486; however, both compounds were more potent in the JURKAT T-cell leukaemia line.

Table 1 also shows the relative potencies of Pim-1 inhibitors in comparison to conventional cytotoxic anti-cancer drugs in a number of cell lines derived from solid tumours. The data was obtained following a 96-hour exposure of cells to cytotoxic drugs of Pim-1 inhibitors. Shorter incubation (24-hour) with the Pim-1 inhibitors did not alter the efficacy, although the potencies of each compound were marginally reduced (data not shown). The Pim-1 inhibitors are regarded as cytostatic agents and therefore, the longer incubation period was chosen for comparison to the effects of cytotoxic anti-cancer drugs.

As expected, the various anti-cancer drugs displayed considerable variation in the IC_{50} values for cytotoxicity, with a rank order of potency of: VLB>DOX/MIT>ETO>CPL. The anti-cancer drugs displayed potencies in the nanomolar range; with the exception of cisplatin, which was effective at micromolar concentrations. Both Pim-1 inhibitors also displayed potency values in the low micromolar range in all cell lines tested. In addition, there were no significant differences in the potency of Pim-1 inhibitors between leukaemia and solid tumour cell lines.

The primary focus of the investigation was to examine the relative efficacy of Pim-1 inhibitors between drug sensitive and multidrug resistant cells expressing the ABC transporter ABCG2. The breast cancer cell line $MCF7^{WT}$ was exposed to increasing concentrations of flavopiridol to select for drug resistant cells as described [2]. The resultant drug-resistant cell line is referred to as $MCF7^{FLV1000}$ and, as shown in figure 2, the observed drug resistance is

most likely associated with expression of ABCG2. Furthermore, the cell line displays expression of the 45kD and the 33kD isoforms of Pim-1 kinase. The parental MCF7^{WT} cell line does not express ABCG2; however it does express both PIM1 isoforms (data not shown). Figure 3a demonstrates that K00135 produces growth inhibitory effects on the MCF7^{WT} (IC_{50} = 2.7±0.5 μM) and MCF7^{FLV1000} cell lines (IC_{50} = 1.1±0.3 μM). The small differences in relative Pim-1 inhibitor in sensitivity of the two cell lines were not statistically significant, although the data were described by different relationships. Curve-fitting of the variable slope and unity slope dose-response relationships were compared using an F-test. A variable slope equation provided the most suitable (F-test; P<0.001) fit to the experimental data with MCF7^{WT} cells characterised by a slope of -2.6; whereas the MCF7 ^{FLV1000} cells were best described by the equation with a slope of 1.0. Data for the effects of K00486 on the growth of both cell lines are shown in Figure 3b. K00486 inhibited growth of MCF7^{WT} cells with an IC_{50} of 1.9±0.2 μM and with an IC_{50} of 2.6±0.1 μM in the MCF7^{FLV1000} cells. The experimental data in the parental cells was again best described with a variable slope (F-test; P<0.0001) with a value of -4.4.

Inhibition of Pim-1 leads to growth inhibition of a number of leukaemic and solid tumour cell lines, albeit with potencies lower than conventional genotoxic anticancer drugs. In addition, the Pim inhibitors displayed equipotency in drug sensitive and resistant cells, the latter expressing ABCG2. The lack of any significant difference in potency between the two cell lines suggests that the compounds are not substrates for transport by ABCG2.

3.2 The efficacy of Pim-1 inhibitors on the growth of multidrug resistant cancer cell lines

The ability of Pim-1 inhibitors to produce growth inhibition even in drug resistant cell lines suggests that they may facilitate the activity of conventional anti-cancer drugs. Therefore, the potency and efficacy of a series of genotoxic anti-cancer drugs in the absence or presence of Pim-1 inhibitors were assessed in MCF7 and MCF7^{FLV1000} cells. Dose-response analysis was used to generate an IC_{50} for the anti-cancer drug and the degree of resistance calculated (Table 2). The concentrations of Pim-1 inhibitors used were lower than the IC_{50} values obtained for their ability to effect cell growth when added alone.

The cyclin kinase inhibitor Flavopridol inhibited growth of the parental MCF7 cell line with an IC_{50} of 52.6±7.3nM and the potency was reduced to 2017±78nM in the ABCG2 expressing

$MCF7^{FLV1000}$ cells. The ratio of IC_{50} values indicates that the level of resistance to this drug was 38-fold. In the presence of the ABCG2 inhibitor FTC (0.3μM), there was no significant effect on potency in MCF7 cells; however, the IC_{50} value was reduced to 193±30nM in the resistant line. The reduced potency revealed a significant reduction in the level of resistance to 4.5-fold by inhibiting the activity of ABCG2. Addition of Pim1 inhibitors also caused significant increases in the potency of Flavipiridol and in each case reducing the level of drug resistance. Neither compound altered the efficacy or potency of Flavopiridol to generate growth inhibition in the drug sensitive MCF7 cells.

Mitoxantrone, a Topoisomerase II inhibitor, also displayed reduced potency in drug resistant $MCF7^{FLV1000}$ cells (IC_{50} = 525±69nM) compared to the parental MCF7 cells (IC_{50} = 12.9±3.1nM). This 40-fold resistance to mitoxantrone was reduced to 15-fold by 0.3μM FTC. In the $MCF7^{FLV1000}$ cells the Pim1 inhibitor K00135 reduced the level of mitoxantrone resistance to 24-fold at a concentration of 0.1μM (IC_{50} = 209±51nM) and a further reduction to 13-fold at a concentration of 0.3μM (IC_{50} = 81±21nM). Similar reductions in mitoxantrone resistance were obtained for K00486, although the concentrations used to achieve this were higher. Once again, there were no effects of Pim-1 inhibitors on the growth of MCF7 cells.

The greatest level of drug resistance observed in the $MCF7^{FLV1000}$ cells (336-fold) was conferred against the Topoisomerase I inhibitor Topotecan. The potency of Topotecan was improved from IC_{50} = 2736±127nM to IC_{50} = 163±27nM in the presence of 0.3μM FTC, which represents a reduction in the level of resistance to 35-fold. The Pim-1 inhibitor K00486 (1.0μM) also reduced the level of Topotecan resistance to 35-fold and improved the potency of the cytotoxic drug to 177±13nM. K00135 also improved the potency of Topotecan, although the level of improvement was not as large as observed for K00486 at the concentrations tested.

The well-characterised R482G mutant isoform of ABCG2 imparts a number of changes in the cross-resistance pattern compared to the wild-type isoform. The latter has a considerably lower degree of resistance to the widely used anthracycline doxorubicin. Table 2 demonstrates that the degree of resistance in $MCF7^{FLV1000}$ cells compared to their parental control was only 8-fold, which was lower than the other compounds tested. Nonetheless, the degree of resistance was reduced to 3-fold by the ABCG2 inhibitor FTC at a concentration of 0.3μM. Both K00135 and K00486 were able to potentiate the cytotoxicity of

doxorubicin in the MCF7^{FLV1000} cells, but not the parental control.

The data in Table 2 demonstrate that expression of ABCG2 confers resistance to a number of anti-cancer drugs and that pharmacological inhibition of this transporter can overcome the phenotype. More importantly, inhibitors of Pim-1 also produce a dose dependent reduction in the degree of resistance by augmenting the potency of each of the anti-cancer drugs tested. The mechanism underlying how Pim-1 inhibitors improve the potency of anti-cancer drugs requires further investigation.

The ability of K00135 and K00486 to overcome multidrug resistance in cells expressing ABCB1 was assessed using a similar strategy. As shown in Table 3, the NCI$^{ADR/Res}$ cell line that expresses ABCB1 displayed considerable resistance (526-fold) to doxorubicin compared to the parental MCF7 cells. The ABCB1 inhibitor verapamil (3μM) increased the potency of doxorubicin from IC_{50} = 2736±127nM to IC_{50} = 86±14nM ($P<0.05$), exclusively in the drug resistant cells. This represents a reduction in the degree of resistance from 526- to 32-fold. However, the addition of Pim-1 inhibitors did not cause any alteration in the potency of doxorubicin or the degree of resistance. This indicates that the two compounds K00135 and K00486 produced inhibition specific to ABCG2 and not ABCB1.

3.3 The effects of Pim-1 inhibitors on the steady-state accumulation of [^{3}H]-Mitoxantrone in MCF7^{FLV1000} cells

The Pim1 inhibitors were shown in the previous section to overcome drug resistance to a number of anticancer drugs in cell lines selected for resistance to flavopiridol. The drug resistance is primarily due to over-expression of the ABC transporter ABCG2. Consequently, the mechanism underlying the circumvention of drug resistance by the inhibitors is likely to involve altered accumulation of anti-cancer drugs. To investigate this mechanistic issue, the steady-state accumulation of the ABCG2 substrate [^{3}H]-mitoxantrone was investigated in the two cell lines. Initially, the accumulation was measured in the presence, or absence, of the specific ABCG2 inhibitor FTC as shown in Figure 4a. An incubation period of 3 hours was required to achieve steady-state accumulation of the radiolabelled drug at a total concentration of 1μM. The accumulation of [^{3}H]-mitoxantrone in MCF7 cells was 2.44±0.22 pmol mg^{-1} in the absence of FTC and the value was 1.47±0.15 pmol mg^{-1} in MCF7^{FLV1000} cells, which represents a statistically significant difference ($P<0.005$). The addition of increasing concentrations of FTC (0.5-10μM) did not alter the of [^{3}H]-mitoxantrone in the

MCF7 cells since the level at the highest FTC concentration (2.62±0.21 pmol mg^{-1}) was not significantly different from the control value. In contrast, the ABGC2 inhibitor produced a dose-dependent increase in the accumulation of [^{3}H]-mitoxantrone in MCF7^{FLV1000} cells to a level (2.61±0.36 pmol mg^{-1} at 10μM FTC) that was identical to the sensitive MCF7 cells.

Identical analysis was undertaken to assess the ability of Pim inhibitors to modulate the steady-state accumulation of [^{3}H]-mitoxantrone. In addition, the investigations were done for multiple pre-incubation times (0, 21, 45 and 69 hr) for cells with each of the Pim-1 inhibitors and the data shown in Figure 4b-c. The data were normalised to the level of [^{3}H]-mitoxantrone accumulation observed in the absence of Pim-1 inhibitor, which was set to a value of 1.0. The increased exposure to Pim-1 inhibitors reveals any long-term cellular effects on the activity or expression of Pim-1 kinase.

Figure 4b demonstrates that the addition of K00135 did not result in any alteration of [^{3}H]-mitoxantrone accumulation in the MCF7 cell line, regardless of the incubation time. In contrast, the addition of K00135 (2μM) produced a 2.6-fold increase of the steady-state accumulation of [^{3}H]-mitoxantrone in MCF7^{FLV1000} cells without any pre-incubation. As mentioned earlier, the assay time to reach steady-state accumulation of radiolabel was 3 hr. This result in MCF7^{FLV1000} cells suggests a direct effect on the activity of ABCG2. Extended pre-incubation of these cells with K00135 produced a significant, and time-dependent, increase in the accumulation of [^{3}H]-mitoxantrone. This data suggests that the compound also produces an additional long-term effect on ABCG2 activity resulting from inhibition of Pim-1 kinase.

Figure 4c shows the effects of K00486 (2μM) on [^{3}H]-mitoxantrone accumulation in the two cell lines. Similarly, the Pim-1 inhibitor did not generate any significant alterations in radiolabel accumulation in the drug sensitive MCF7 cells. However, there were time dependent alterations of [^{3}H]-mitoxantrone in the drug resistant MCF7^{FLV1000} cells. The accumulation was increased 1.9-fold where there was no pre-incubation with K00486 and following a 69 hr pre-incubation the level had been increased over 5-fold.

[^{3}H]-Mitoxantrone accumulation was also increased using a higher concentration of Pim1 inhibitors (i.e. 4μM); however this did not differ markedly from the observations reported for the lower concentration (data not shown).

In summary, the Pim-1 inhibitors appear to display both short- and long-term effects on the

accumulation of the ABCG2 substrate [^{3}H]-mitoxantrone in the MCF7^{FLV1000} cell line. There were no effects in the drug sensitive MCF7 cells, suggesting that this effect was specifically related to ABCG2. Short-term effects are likely to involve direct inhibition of the protein although the 3 hour duration of this assay does not entirely rule out post-translational effects. The long-term effects are likely to involve altered expression and/or post-translational modification of ABCG2.

3.4 The effects of Pim1 inhibitors on total expression of ABCG2 in MCF7^{FLV1000} cells

The ability of the Pim-1 inhibitors to alter the expression of ABCG2 was investigated by western blot analysis on MCF7^{FLV1000} cells following incubation with the compounds for 8 days. Data on the expression levels of ABCG2 are shown in figure 5.

Figure 5a demonstrates a representative western immuno-blot of ABCG2 expression for MCF7^{FLV1000} cells in the absence or presence of 4μM K00486 over an eight day period. The intensity of ABCG2 bands were quantified using densitometry and the results from four preparations expressed as a function of culture time (Figure 5b). The initial time point was obtained 24-hour following cell seeding and displayed low level ABCG2 expression. During the eight day culture period, the expression of ABCG2 increased five to six-fold in the MCF7^{FLV1000} cells. In contrast, in the presence of Pim-1 inhibitors the expression of ABCG2 did not alter significantly during this period and remained similar at day 8 compared to day 0.

The expression data reveal a considerable reduction in the levels of ABCG2 in MCF7^{FLV1000} cells following the addition of Pim-1 inhibitors. Thus, the ability of these compounds to overcome drug resistance is also related to the progressive diminution of ABCG2 expression. This effect is in addition to the ability to interact directly with ABCG2 and thereby impair cytotoxic drug efflux.

4. DISCUSSION

The investigation has revealed that multidrug resistance conferred by ABCG2 was overcome by two imidazo-pyridazine derivatives, which had previously been developed as specific inhibitors of the serine/threonine kinase Pim-1. Earlier studies have demonstrated that co-expression of Pim-1 and ABCG2 produces increased resistance and that the proteins share a physical interaction. Both inhibitors overcame ABCG2 mediated resistance by modulating transport of the substrate mitoxantrone. Further investigation on the transport process revealed a longer-term effect that was associated with reduced expression of ABCG2 in the cancer cell lines. This two-pronged approach provides a novel alternative to the classical approach of exclusively targeting the transporter. Potent and selective modulation of regulatory kinase proteins alleviates the problems with developing specific inhibitors of polyspecific drug transporters such as ABCG2.

Amongst the earliest reports on the function of Pim-kinase were the observations that the protein weakly transformed mesenchymal cells to generate lymphoma and leukaemia [27, 28]. Furthermore, elevated expression of Pim-kinase was observed in human myeloid leukaemia and lymphoma [29, 30]. As the biology of the kinase became more widely investigated, a role in solid tumours became apparent, with expression demonstrated in prostate, gastric, hepatic, bladder and colorectal tumours [16, 31-33]. The tumour growth stimulating properties of Pim-kinase [34, 35] render the protein a target for therapeutic intervention in cancer. The present investigation demonstrated growth inhibition of a panel of cancer cell lines derived from haematological malignancies and solid tumours by two potent imidazo-pyridazine based inhibitors of Pim-kinase. This efficacy further supports an inherent role for Pim-kinases in tumour biology. The potency of the Pim inhibitors to produce growth inhibition was in the low micromolar range, which was similar to cisplatin, but lower than most cytotoxic chemotherapy drugs.

In the last decade medicinal chemistry efforts have generated several classes of Pim-kinase inhibitors [36, 37]. The “boom” in production of inhibitor compounds has benefited from the availability of high resolution structural data for Pim-kinases [24]. For example, the K00135 inhibitor used in the present study co-crystallises with Pim-1 and numerous derivatives have been developed from knowledge of the molecular interactions underpinning binding [24].

The ABCG2 expressing cells displayed considerable differences in the level of resistance to

a range of anti-cancer drugs and other compounds, as shown in Table 1 in the review by Nakanashi *et al* [38]. The range of resistance (and the relative order) to anticancer drugs in the current investigation is in broad agreement with previous work using the MCF7^{FLV1000} cell line [2]. The mycotoxin FTC was one of the first inhibitors of ABCG2 to be identified by virtue of its ability to restore sensitivity of drug resistant cell lines to Topotecan, mitoxantrone and doxorubicin [39]. The potency of FTC to overcome ABCG2 mediated resistance was in the range 0.1-5μM. In the present investigation a fixed concentration of FTC (0.3μM) produced a reduction in the extent of resistance by a factor of up to 10-fold and thereby restored sensitivity to anticancer drugs to levels similar to the MCF7 cell line.

Both Pim-kinase inhibitors, at concentrations of 0.1-1μM, were able to reduce the extent of resistance to anti-cancer drugs in the MCF7^{FLV1000} cell line. Furthermore, the potencies and efficacies were similar to that of FTC. The potencies of K00135 and K00486 to inhibit Pim-1 kinase have been demonstrated as 0.12 and 0.04μM respectively, whereas the potency to inhibit Pim-2 kinase was reduced by up to 50-fold [24]. In addition, the potencies to overcome the resistant phenotype in ABCG2 expressing cells were similar to another imidazo-pyridazine compound SGI-1776, which reached stage clinical trials [40].

This data clearly indicates that inhibition of Pim-kinase can overcome the resistant phenotype produced by expression of ABCG2 and the subsequent focus was to ascertain the underlying mechanism.

In contrast to the inhibitor SGI-1776, which was able to inhibit and overcome the actions of ABCB1 in cancer cell lines [40], K00135 and K00486 were selective for ABCB1. However, SGI-1776 differs markedly in chemical structure from K00135/K00486, despite the common imidazo-pyridazine moiety. It is therefore likely that the different substituents in SGI-1776 enhance its ability to interact directly with ABCB1.

It has been widely demonstrated that ABCG2 confers resistance in the MCF7^{FLV1000} cell line by preventing accumulation of drugs such as mitoxantrone [2, 39]. The assay required a long incubation period (i.e. 3hr) in order that the accumulation of [^{3}H]-mitoxantrone reached a steady-state, which is in agreement with previous studies [2, 39]. The addition of both Pim-kinase inhibitors increased the extent of mitoxantrone accumulation, which suggests a direct interaction between the Pim-inhibitors and ABCG2. SGI-1776 was shown to produce similar effects on mitoxantrone accumulation in ABCG2 expressing cells [40]. Classically, inhibitors

of multidrug efflux pumps from the ABC family have been generated to interact with the drug binding site and thereby reduce the rate of substrate translocation. However, the Pim inhibitors used in this study were designed to bind at the catalytic domain of the kinase. The Pim-1 protein has an ATP binding domain that is distinct from most kinases [24, 36]. Structural data demonstrated that K00135/K00486 do not bind to the "kinase hinge region" as predicted, but to the novel N-terminal helix within the catalytic region. Therefore, although they interact at the ATP binding domain, they are not considered ATP mimetics. Consequently, this provides a high selectivity for the catalytic domain of Pim proteins and only interacted with one other protein from a panel of over fifty Ser/Thr-kinases [24]. Therefore, it is highly unlikely that K00135/K00486 interact with the ATP binding domain of ABC transporters such as ABCG2. Any direct interaction is more likely to occur at the substrate binding domain.

The longer-term effects of the Pim-kinase inhibitors will likely involve the interaction between this regulatory protein and ABCG2, presumably at the post-translational level. An investigation by Xie et al [13] provided considerable evidence regarding the interaction between Pim-1 and ABCG2. For example, the two proteins are co-expressed in several drug resistant cell lines and co-localise at the plasma membrane. The investigation also suggested that Threonine-362 in ABCG2 was phosphorylated by Pim-1. Knocking-down the expression of Pim-1 reduced the oligomerisation of ABCG2, which rendered the cells sensitive to mitoxantrone and doxorubicin. This suggests that Pim-1 is an important factor in the multidrug resistant phenotype conferred by ABCG2. This confirms our observation that pharmacological inhibition of Pim-kinase is able to overcome ABCG2 mediated resistance. Moreover, it supports the proposal that the progressive, or long-term, effects of Pim-kinase inhibition on [^{3}H]-mitoxantrone accumulation may be due to disruption of the stability of ABCG2 at the plasma membrane.

During the growth of MCF7^{FLV1000} cells the levels of ABCG2 increased in a hyperbolic manner. In the presence of both compounds the extent of this increase was severely reduced and therefore, Pim-kinase inhibition was associated with a significant reduction in expression of ABCG2. Treatment of cancer cells with another Pim-kinase inhibitor, SGI-1776, also reduced the surface expression of ABCG2 [40], supporting a key regulatory interaction between the two proteins.

Control of ABC transporter expression is remarkably complex, involves numerous over-

lapping pathways and is frequently cell, or tissue, specific [38, 41]. ABCG2 expression has been intensively investigated in recent years, with contributions at the level of epigenetics, post-transcriptional regulation and post-translational modification (for review see [38]). Two of the most frequently observed control factors for ABCG2 expression are Pim-kinase and the PI3K/Akt signalling pathway [13, 14, 25]. Moreover, these two pathways have been demonstrated to interact in a synergistic manner [42] to promote cell growth and engender an anti-apoptotic cellular environment. In addition, inhibition of BCR-ABL by Imatinib in resistant K562 leukaemic cells was associated with post-transcriptional regulation of ABCG2 expression via PI3K/Akt [43]. It is tempting to speculate that the K00135/K00486 mediated reduction of ABCG2 expression involves the co-ordinated effects of Pim-kinase and the PI3K/Akt pathway at post-translational and/or post-transcriptional levels. The pathway or mechanism of interaction and synergy between these two factors remains to be established to date.

The data indicate that Pim-kinase inhibition by the two imidazo-pyridazine compounds is able to circumvent ABCG2 mediated multidrug resistance. The mechanism underlying this effect is by reducing the expression level of ABCG2 in the cells. This indicates that phosphorylation of ABCG2 is important in the stability of the protein at the plasma membrane. Moreover it provides further proof that the drug resistant phenotype may be circumvented or overcome via modulation of regulatory protein activity and in the case of ABCG2, Pim-kinase is a key target.

5. ACKNOWLEDGEMENTS

This investigation was funded by a project grant (090072/Z/09/Z) from the Wellcome Trust awarded to Richard Callaghan, Stefan Knapp and Ian Kerr. SK is grateful for support by the SGC, a registered charity (number 1097737) that receives funds from AbbVie, Bayer, Boehringer Ingelheim, the Canada Foundation for Innovation, the Canadian Institutes for Health Research, Genome Canada, GlaxoSmithKline, Janssen, Lilly Canada, the Novartis Research Foundation, the Ontario Ministry of Economic Development and Innovation, Pfizer, Takeda, and the Wellcome Trust [092809/Z/10/Z].

6. REFERENCES

1. Doyle LA, Yang WD, Abruzzo LV, Krogmann T, Gao YM, Rishi AK & Ross DD (1998) A multidrug resistance transporter from human MCF-7 breast cancer cells. *Proceedings of the National Academy of Sciences of the United States of America* **95**, 15665-15670.

2. Robey RW, Medina-Perez WY, Nishiyama K, Lahusen T, Miyake K, Litman T, Senderowicz AM, Ross DD & Bates SE (2001) Overexpression of the ATP-binding cassette half-transporter, ABCG2 (MXR/BCRP/ABCP1), in flavopiridol-resistant human breast cancer cells. *Clinical Cancer Research* **7**, 145-152.

3. Fellner S, Bauer B, Miller DS, Schaffrik M, Fankhanel M, Spruss T, Bernhardt G, Graeff C, Farber L, Gschaidmeier H, et al. (2002) Transport of paclitaxel (Taxol) across the blood-brain barrier in vitro and in vivo. *Journal of Clinical Investigation* **110**, 1309-1318.

4. Robey RW, Polgar O, Deeken J, To KW & Bates SE (2007) ABCG2: determining its relevance in clinical drug resistance. *Cancer and Metastasis Reviews* **26**, 39-57.

5. Ross DD, Wooten PJ, Tong Y, Cornblatt B, Levy C, Sridhara R, Lee EJ & Schiffer CA (1994) Synergistic Reversal of Multidrug-Resistance Phenotype in Acute Myeloid-Leukemia Cells by Cyclosporine-a and Cremophor El. *Blood* **83**, 1337-1347.

6. Scheffer GL, Maliepaard M, Pijnenborg ACLM, van Gastelen MA, de Jong MC, Schroeijers AB, van der Kolk DM, Allen JD, Ross DD, van der Valk P, et al. (2000) Breast cancer resistance protein is localized at the plasma membrane in mitoxantrone- and topotecan-resistant cell lines. *Cancer Research* **60**, 2589-2593.

7. Ozvegy C, Litman T, Szakacs G, Nagy Z, Bates S, Varadi A & Sarkadi B (2001) Functional characterization of the human multidrug transporter, ABCG2, expressed in insect cells. *Biochemical and Biophysical Research Communications* **285**, 111-117.

8. McDevitt CA, Collins RF, Conway M, Modok S, Storm J, Kerr ID, Ford RC & Callaghan R (2006) Purification and 3D structural analysis of oligomeric human multidrug transporter ABCG2. *Structure* **14**, 1623-1632.

9. Diop NK & Hrycyna CA (2005) N-linked glycosylation of the human ABC transporter ABCG2 on asparagine 596 is not essential for expression, transport activity, or trafficking to the plasma membrane. *Biochemistry* **44**, 5420-5429.

10. Henriksen U, Fog JU, Litman T & Gether U (2005) Identification of intra- and intermolecular disulfide bridges in the multidrug resistance transporter ABCG2. *Journal of Biological Chemistry* **280**, 36926-36934.

11. Polgar O, Robey RW, Morisaki K, Dean M, Michejda C, Sauna ZE, Ambudkar SV, Tarasova N & Bates SE (2004) Mutational analysis of ABCG2: Role of the GXXXG motif. *Biochemistry* **43**, 9448-9456.

12. Takada T, Suzuki H, Gotoh Y & Sugiyama Y (2005) Regulation of the cell surface expression of human BCRP/ABCG2 by the phosphorylation state of Akt in polarized cells. *Drug Metabolism and Disposition* **33**, 905-909.

13. Xie Y, Xu K, Linn DE, Yang X, Guo Z, Shimelis H, Nakanishi T, Ross DD, Chen H,

Fazli L, et al. (2008) The 44-kDa pim-1 kinase phosphorylates BCRP/ABCG2 and thereby promotes its multimerization and drug-resistant activity in human prostate cancer cells. *Journal of Biological Chemistry* **283**, 3349-3356.

14. Mogi M, Yang J, Lambert JF, Colvin GA, Shiojima I, Skurk C, Summer R, Fine A, Quesenberry PJ & Walsh K (2003) Akt signaling regulates side population cell phenotype via Bcrp1 translocation. *Journal of Biological Chemistry* **278**, 39068-39075.

15. Krishnan N, Pan HQ, Buckley DJ & Buckley AR (2003) Prolactin-regulated pim-1 transcription. *Endocrine* **20**, 123-129.

16. Shah N, Pang B, Yeoh KG, Thorn S, Chen CS, Lilly MB & Salto-Tellez M (2008) Potential roles for the PIM1 kinase in human cancer - A molecular and therapeutic appraisal. *European Journal of Cancer* **44**, 2144-2151.

17. Saris CJM, Domen J & Berns A (1991) The Pim-1 Oncogene Encodes 2 Related Protein-Serine Threonine Kinases by Alternative Initiation at Aug and Cug. *Embo Journal* **10**, 655-664.

18. Leverson JD, Koskinen PJ, Orrico FC, Rainio EM, Jalkanen KJ, Dash AB, Eisenman RN & Ness SA (1998) Pim-1 kinase and p100 cooperate to enhance c-myb activity. *Molecular Cell* **2**, 417-425.

19. Mochizuki T, Kitanaka C, Noguchi K, Muramatsu T, Asai A & Kuchino Y (1999) Physical and functional interactions between Pim-1 kinase and Cdc25A phosphatase - Implications for the Pim-1-mediated activation of the c-Myc signaling pathway. *Journal of Biological Chemistry* **274**, 18659-18666.

20. Koike N, Maita H, Taira T, Ariga H & Iguchi-Ariga SMM (2000) Identification of heterochromatin protein 1 (HP1) as a phosphorylation target by Pim-1 kinase and the effect of phosphorylation on the transcriptional repression function of HP1. *Febs Letters* **467**, 17-21.

21. Xie XM, Zhao XQ, Liu YF, Zhang JF, Matusik RJ, Slawin KM & Spencer DM (2001) Adenovirus-mediated tissue-targeted expression of a Caspase-9-based artificial death switch for the treatment of prostate cancer. *Cancer Res* **61**, 6795-6804.

22. Palaty CK, ClarkLewis I, Leung D & Pelech SL (1997) Phosphorylation site substrate specificity determinants for the Pim-1 protooncogene-encoded protein kinase. *Biochemistry and Cell Biology-Biochimie Et Biologie Cellulaire* **75**, 153-162.

23. Mumenthaler SM, Ng PYB, Hodge A, Bearss D, Berk G, Kanekal S, Redkar S, Taverna P, Agus DB & Jain A (2009) Pharmacologic inhibition of Pim kinases alters prostate cancer cell growth and resensitizes chemoresistant cells to taxanes. *Molecular Cancer Therapeutics* **8**, 2882-2893.

24. Pogacic V, Bullock AN, Fedorov O, Filippakopoulos P, Gasser C, Biondi A, Meyer-Monard S, Knapp S & Schwaller J (2007) Structural analysis identifies imidazo[1,2-b]Pyridazines as PIM kinase inhibitors with In vitro antileukemic activity. *Cancer Research* **67**, 6916-6924.

25. Isaac M, Siu A & Jongstra J (2011) The oncogenic PIM kinase family regulates drug resistance through multiple mechanisms. *Drug Resistance Updates* **14**, 203-211.

26. Rivers F, O'Brien TJ & Callaghan R (2008) Exploring the possible interaction between anti-epilepsy drugs and multidrug efflux pumps; in vitro observations. *Eur J Pharmacol* **598**, 1-8.

27. Moroy T, Grzeschiczek A, Petzold S & Hartmann KU (1993) Expression of a Pim-1 transgene accelerates lymphoproliferation and inhibits apoptosis in lpr/lpr mice. *Proc Natl Acad Sci U S A* **90**, 10734-10738.

28. Moroy T, Verbeek S, Ma A, Achacoso P, Berns A & Alt F (1991) E mu N- and E mu L-myc cooperate with E mu pim-1 to generate lymphoid tumors at high frequency in double-transgenic mice. *Oncogene* **6**, 1941-1948.

29. Nieborowska-Skorska M, Hoser G, Kossev P, Wasik MA & Skorski T (2002) Complementary functions of the antiapoptotic protein A1 and serine/threonine kinase pim-1 in the BCR/ABL-mediated leukemogenesis. *Blood* **99**, 4531-4539.

30. Selten G, Cuypers HT & Berns A (1985) Proviral activation of the putative oncogene Pim-1 in MuLV induced T-cell lymphomas. *EMBO J* **4**, 1793-1798.

31. Bachmann M & Moroy T (2005) The serine/threonine kinase Pim-1. *Int J Biochem Cell Biol* **37**, 726-730.

32. Guo S, Mao X, Chen J, Huang B, Jin C, Xu Z & Qiu S (2010) Overexpression of Pim-1 in bladder cancer. *J Exp Clin Cancer Res* **29**, 161.

33. Mumenthaler SM, Ng PY, Hodge A, Bearss D, Berk G, Kanekal S, Redkar S, Taverna P, Agus DB & Jain A (2009) Pharmacologic inhibition of Pim kinases alters prostate cancer cell growth and resensitizes chemoresistant cells to taxanes. *Mol Cancer Ther* **8**, 2882-2893.

34. Wang Z, Bhattacharya N, Weaver M, Petersen K, Meyer M, Gapter L & Magnuson NS (2001) Pim-1: a serine/threonine kinase with a role in cell survival, proliferation, differentiation and tumorigenesis. *J Vet Sci* **2**, 167-179.

35. White E (2003) The pims and outs of survival signaling: role for the Pim-2 protein kinase in the suppression of apoptosis by cytokines. *Genes Dev* **17**, 1813-1816.

36. Qian KC, Wang L, Hickey ER, Studts J, Barringer K, Peng C, Kronkaitis A, Li J, White A, Mische S, et al. (2005) Structural basis of constitutive activity and a unique nucleotide binding mode of human Pim-1 kinase. *J Biol Chem* **280**, 6130-6137.

37. Swords R, Kelly K, Carew J, Nawrocki S, Mahalingam D, Sarantopoulos J, Bearss D & Giles F (2011) The Pim kinases: new targets for drug development. *Curr Drug Targets* **12**, 2059-2066.

38. Nakanishi T & Ross DD (2012) Breast cancer resistance protein (BCRP/ABCG2): its role in multidrug resistance and regulation of its gene expression. *Chin J Cancer* **31**, 73-99.

39. Rabindran SK, Ross DD, Doyle LA, Yang W & Greenberger LM (2000) Fumitremorgin C reverses multidrug resistance in cells transfected with the breast cancer resistance protein. *Cancer Res* **60**, 47-50.

40. Natarajan K, Bhullar J, Shukla S, Burcu M, Chen ZS, Ambudkar SV & Baer MR (2013) The Pim kinase inhibitor SGI-1776 decreases cell surface expression of P-glycoprotein (ABCB1) and breast cancer resistance protein (ABCG2) and drug transport by Pim-1-

dependent and -independent mechanisms. *Biochem Pharmacol* **85**, 514-524.

41. Callaghan R, Crowley E, Potter S & Kerr ID (2008) P-glycloprotein: So many ways to turn it on. *Journal of Clinical Pharmacology* **48**, 365-378.

42. Cen B, Mahajan S, Wang W & Kraft AS (2013) Elevation of receptor tyrosine kinases by small molecule AKT inhibitors in prostate cancer is mediated by Pim-1. *Cancer Res* **73**, 3402-3411.

43. Nakanishi T, Shiozawa K, Hassel BA & Ross DD (2006) Complex interaction of BCRP/ABCG2 and imatinib in BCR-ABL-expressing cells: BCRP-mediated resistance to imatinib is attenuated by imatinib-induced reduction of BCRP expression. *Blood* **108**, 678-684.

7. FIGURE LEGENDS

Figure 1 Pim inhibitor structures

The chemical structures of the Pim1 kinase inhibitors K00135 (*left panel*) and K00486 (*right panel*). The inhibitors were based on the imidazo-[1,2-b]-pyridazine template molecule.

Figure 2 Expression of ABCG2 and Pim-1 in breast cancer cells

Cell lysates were prepared from the drug resistant $MCF7^{FLV1000}$ cell line in 1% SDS and total protein determined colorimetrically. SDS-PAGE (10% gels) and Western blot analysis was done on lysate samples containing 5, 10, 15 & 20μg protein. The *left panel* shows a blot probed with the anti-ABCG2 antibody BXP-21. The arrow indicates the location of the 72kD ABCG2 protein. The blot shown in the *right panel* was probed with the anti-Pim antibody 12H8. The arrows correspond to the 33 and 45kD isoforms of Pim1 kinase. Both proteins were detected using an anti-mouse secondary antibody with subsequent chemiluminescence.

Figure 3 Cytostatic effects of the imidazo-[1,2-b]-pyridazine based Pim1 kinase inhibitors on breast cancer cells

The growth inhibitory effects of (a) K00135 and (b) K00486 were measured in MCF7 (*open symbols, dashed lines*) and $MCF7^{FLV1000}$ (*closed symbols, solid lines*) cell lines. Cells (2.5×10^3 $well^{-1}$) were seeded in 96 well plates and grown with various concentrations (10^{-8}-10^{-4}M) of the inhibitors for 5 days. The cell density following incubation with inhibitors was measured using the Sulforhodamine B assay. The data were fitted with the variable slope dose-response curve using non-linear regression and shown are the mean±SD of three independent experiments.

Figure 4 [^{3}H]-Mitoxantrone accumulation in breast cancer cell lines

(a) MCF7 (*open bars*) and $MCF7^{FLV1000}$ (*filled bars*) grown in 6-well plates were incubated with [^{3}H]-mitoxantrone for 3 hours. Cells were also grown in the presence of varying

concentrations (0.5-10μM) of the ABCG2 inhibitor fumetrimorgen C. Following incubation, the cells were washed, lysed and the amount of [^{3}H]-mitoxantrone determined by scintillation counting.

MCF7 (*open symbols, dashed lines*) and MCF7^{FLV1000} (*filled symbols, solid lines*) grown in 6-well plates were incubated with [^{3}H]-mitoxantrone in the presence or absence of 4μM (b) K00135 or (c) K00486. Cells were pre-incubated with Pim kinase inhibitors for periods shown in the graphs prior to addition of [^{3}H]-mitoxantrone. Following incubation with radiolabel, the cells were washed, lysed and the amount of [^{3}H]-mitoxantrone determined by liquid scintillation counting. Accumulation of [^{3}H]-mitoxantrone was expressed as a fraction of that obtained in the absence of Pim kinase inhibitor in each cell lines.

The data shown represent the mean±SD of three independent experiments.

Figure 5 The effects of Pim1 kinase inhibitors on the expression of ABCG2 in cancer cells

MCF7^{FLV1000} cells were grown in the absence or presence of Pim kinase inhibitors for up to 8 days.

(a) Cell lysates were prepared from the drug resistant MCF7^{FLV1000} cell line in 1% SDS and total protein determined colorimetrically. SDS-PAGE (10% gels) and Western blot analysis was done on lysate samples containing 4μg protein. ABCG2 was detected using the BXP-21 antibody. The *upper panel* shows ABCG2 expression in the absence of inhibitor and the *lower panel* in the presence of 4μM K00486. The panels represent data from a single experiment.

(b) Relative ABCG2 expression was quantified using densitometry and plotted as a function of time in culture. The MCF7^{FLV1000} cells were grown in the presence of DMSO control (*black bars*), 4 μM K00135 (*white bars*) or 4 μM K004865 (*hashed bars*). The data represent mean±SEM from four independent observations.

8. TABLE LEGENDS

Table 1 Effects of Pim-1 inhibitors on the growth of cultured human cancer cells

Cells were seeded at 2 x 10^3 cells per well (total volume = 100μl) in a 96-well tissue culture plate and incubated for 24 hours prior to addition of drugs. Anticancer drugs and the two Pim kinase inhibitors were prepared in medium at twice the desired concentration and 100μl added to each well. Vinblastine was added in the final concentration range 10^{-12}-10^{-5}M and all other drugs in the range 10^{-10}-10^{-4}M. Cells were incubated for 96 hours with the drugs. Cell number and viability was measured with the SRB assay for adherent cultures and with MTS for suspension cultures (i.e. K562 and JURKAT). Cell density was plotted as a function of cytotoxic drug concentration and the IC_{50} values (units shown in parentheses) determined using non-linear regression of the general dose-response equation. The values shown represent mean±SEM from 4-6 independent observations.

Table 2 Effects of Pim-1 inhibitors on anticancer drug efficacy in MCF7 and $MCF7^{FLV1000}$ cells

Cells were seeded at 2 x 10^3 cells per well in a 96-well tissue culture plate and incubated for 24 hours prior to drug addition. Cytotoxic drugs were then added to the cells in the presence or absence of Pim-1 inhibitors and the ABCG2 inhibitor Fumetrimorgen C. The plates were incubated for a further 5 days and the cell density measured using the Sulforhodamine B assay. Cell density was plotted as a function of cytotoxic drug concentration and the IC_{50} values (μM) determined using non-linear regression of the general dose-response equation. The values shown represent mean±SEM from four independent observations. The degree of resistance refers to the ratio of cytotoxic potency in the $MCF7^{FLV1000}$ compared to the MCF7 cells. The symbol (*) represents a statistically significant (P<0.01) difference from the control group (i.e. no Pim-1 or ABCG2 inhibitor). Statistical comparisons were done using ANOVA, with the Bartlett's post-hoc test.

Table 3 Effects of verapamil and Pim-1 inhibitors on anticancer drug efficacy in MCF7 and ABCB1 expressing $NCI^{ADR/Res}$ cell lines

Cells were seeded at 2 x 10^3 cells per well in a 96-well tissue culture plate and incubated for 24 hours prior to drug addition. Cytotoxic drugs were then added to the cells in the presence or absence of Pim-1 inhibitors and the ABCB1 inhibitor Verapamil. The plates were

incubated for a further 5 days and the cell density measured using the SRB assay. Cell density was plotted as a function of cytotoxic drug concentration and the IC_{50} values (nM) determined using non-linear regression of the general dose-response equation. The values shown represent mean±SEM from four independent observations. The degree of resistance refers to the ratio of cytotoxic potency in the $MCF7^{FLV1000}$ compared to the MCF7 cells. The symbol (*) represents a statistically significant ($P<0.01$) difference from the control group (i.e. no Pim-1 or ABCB1 inhibitor). Statistical comparisons were done using ANOVA, with the Bartlett's post-hoc test.

TABLE 1

DRUG	K562	JURKAT	PC3	LNCaP	HT29	H226	DLD1	A549
K00135 (μM)	12±6	2.0±1.1	4.7±2.0	3.9±0.4	19±16	13±5	11±45	28±4
K00486 (μM)	3.9±1.4	1.3±0.5	4.4±1.5	2.0±0.5	11±5	3.8±2.3	4.4±1.7	13±8.
Cisplatin (μM)	5.2±1.8	1.8±0.9	3.8±1.7	12±8	4.7±1.2	14±5	11±6	19±6
Etoposide (nM)	44±8	89±39	287±47	175±25	530±170	102±40	250±119	467±133
Methotrexate (nM)	2.7±0.6	19±9	0.67±0.67	54±19	10±4	41±17	25±9	37±11
Doxorubicin (nM)	3.2±0.8	2.5±0.5	22±4	7.6±2.5	26±10	66±59	9.6±2.3	47±31
Vinblastine (nM)	0.04±0.01	0.038±0.009	0.15±0.07	0.11±0.06	0.31±0.10	0.29±0.14	1.81±0.91	0.76±0.35
Mitoxantrone (nM)	2.6±0.8	0.11±0.07	4.8±1.4	1.6±0.6	6.4±3.4	0.84±0.32	3.2±0.7	2.2±0.3

TABLE 2

CYTOTOXIC DRUG	CELL LINE	CHEMOSENSITISATION AGENT					
		CONTROL	FTC 0.3μM	K00135 0.1μM	K00135 0.3μM	K00486 0.3μM	K00486 1.0μM
	MCF7	52.6±7.3	42.7±5.9	57.7±4.6	52.7±5.9	44.7±6.6	40.4±5.3
Flavopiridol	MCF7^{FLV1000}	2017±78	193±30*	728±87*	201±20*	347±24*	153±11*
	resistance	*38.3*	*4.5*	*12.6*	*3.8*	*7.8*	*3.8*
	MCF7	12.9±3.1	5.9±1.9	8.7±1.8	6.2±0.9	6.3±2.9	6.4±1.7
Mitoxantrone	MCF7^{FLV1000}	525±69	86±4*	209±51*	81±21*	174±49*	35±12*
	resistance	*40.7*	*15.5*	*24.1*	*13.1*	*27.4*	*5.4*
	MCF7	8.1±1.3	4.5±0.4	6.3±0.7	5.2±0.5	6.8±1.1	4.9±0.8
Topotecan	MCF7^{FLV1000}	2736±127	163±27*	1315±86*	353±32*	571±15*	177±13*
	resistance	*336*	*35.9*	*210*	*68.1*	*83.6*	*35.8*
	MCF7	8.5±0.8	9.0±1.2	11.1±0.52	6.6±0.6	12.8±2.1	9.7±1.1
Doxorubicin	MCF7^{FLV1000}	69.9±6.9	29.8±3.7	62.6±3.3*	34.7±4.8*	34±4.2*	24.5±3.6*
	resistance	*8.2*	*3.3*	*5.6*	*5.2*	*2.7*	*2.5*

TABLE 3

CYTOTOXIC DRUG	CELL LINE	CHEMOSENSITISATION AGENT					
		CONTROL	**VERAPAMIL 3μM**	**K00486 0.3μM**	**K00486 1μM**	**K00135 0.1μM**	**K00135 0.3μM**
Doxorubicin	MCF7	4.2±1.4	2.7±0.5	3.3±1.0	4.1±1.0	4.5±1.2	3.4±0.7
	$NCI^{ADR/Res}$	2211±387	86±14*	2076±557	2232±627	2950±780	3094±786
	resistance	*526*	*32*	*629*	*544*	*655*	*910*

FIGURE 1

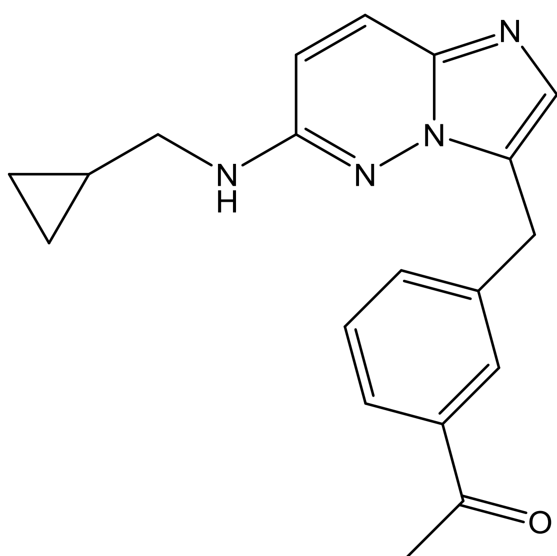

K00135

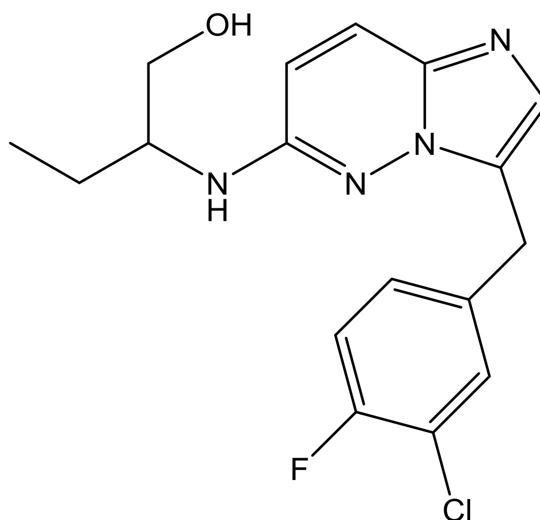

K00486

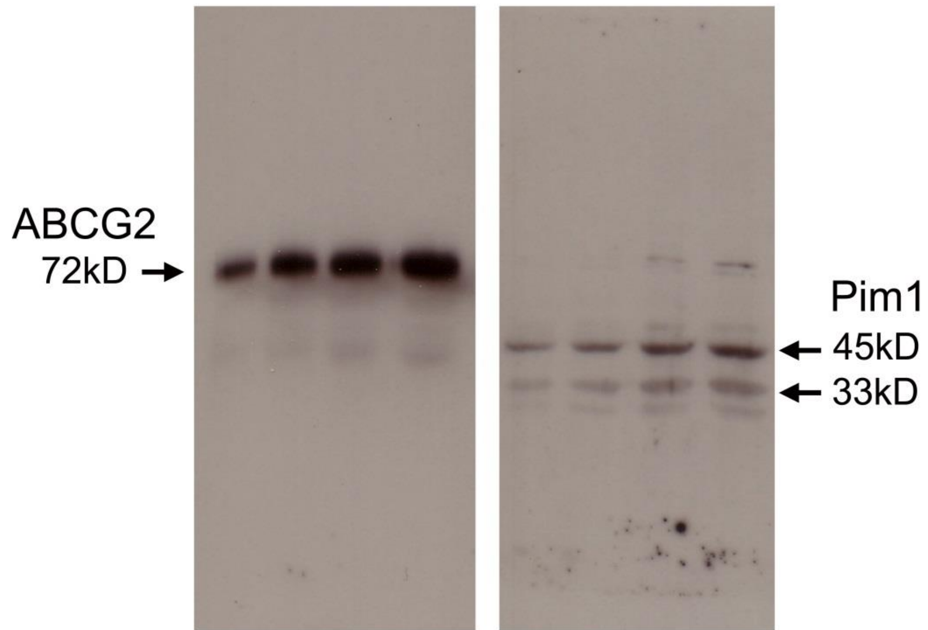

FIGURE 2

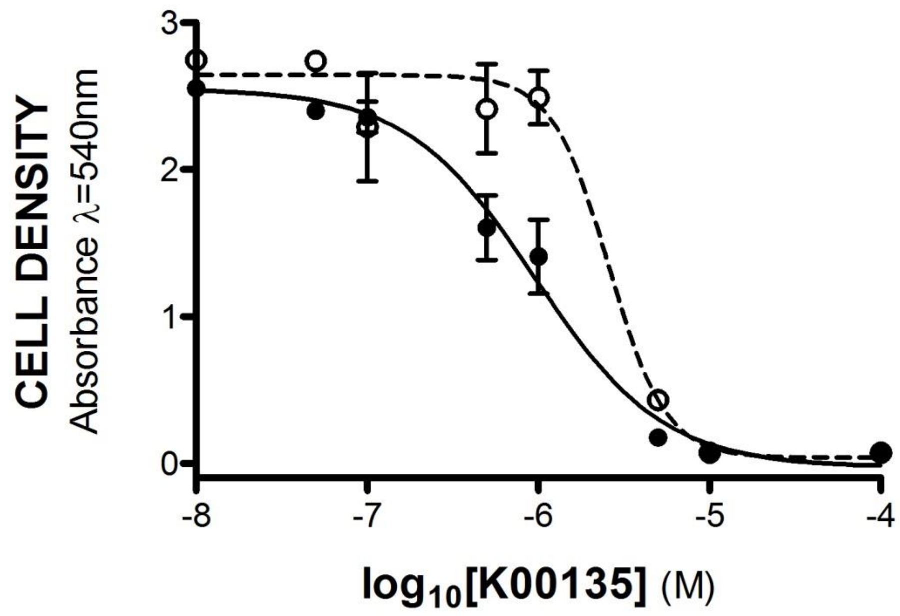

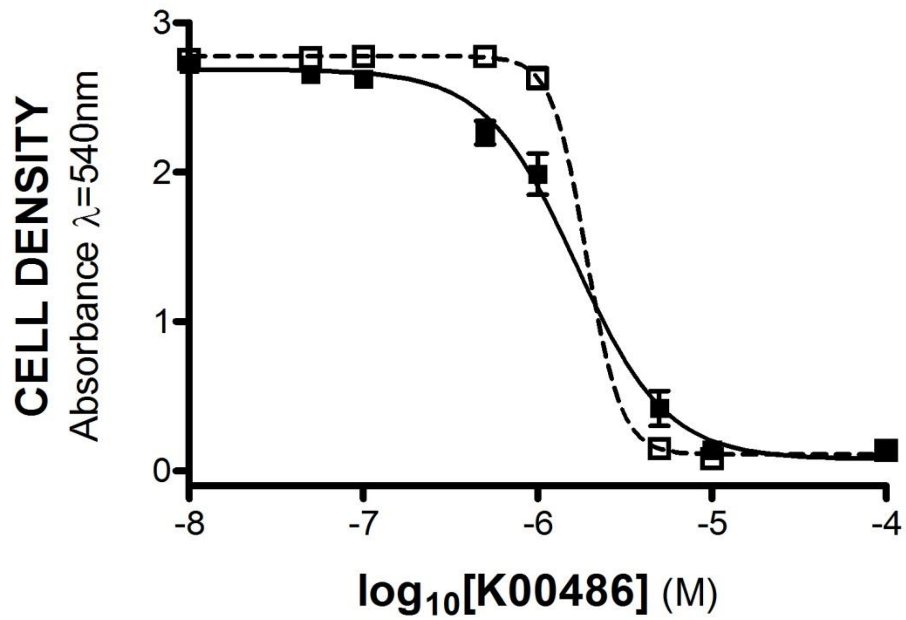

FIGURE 3

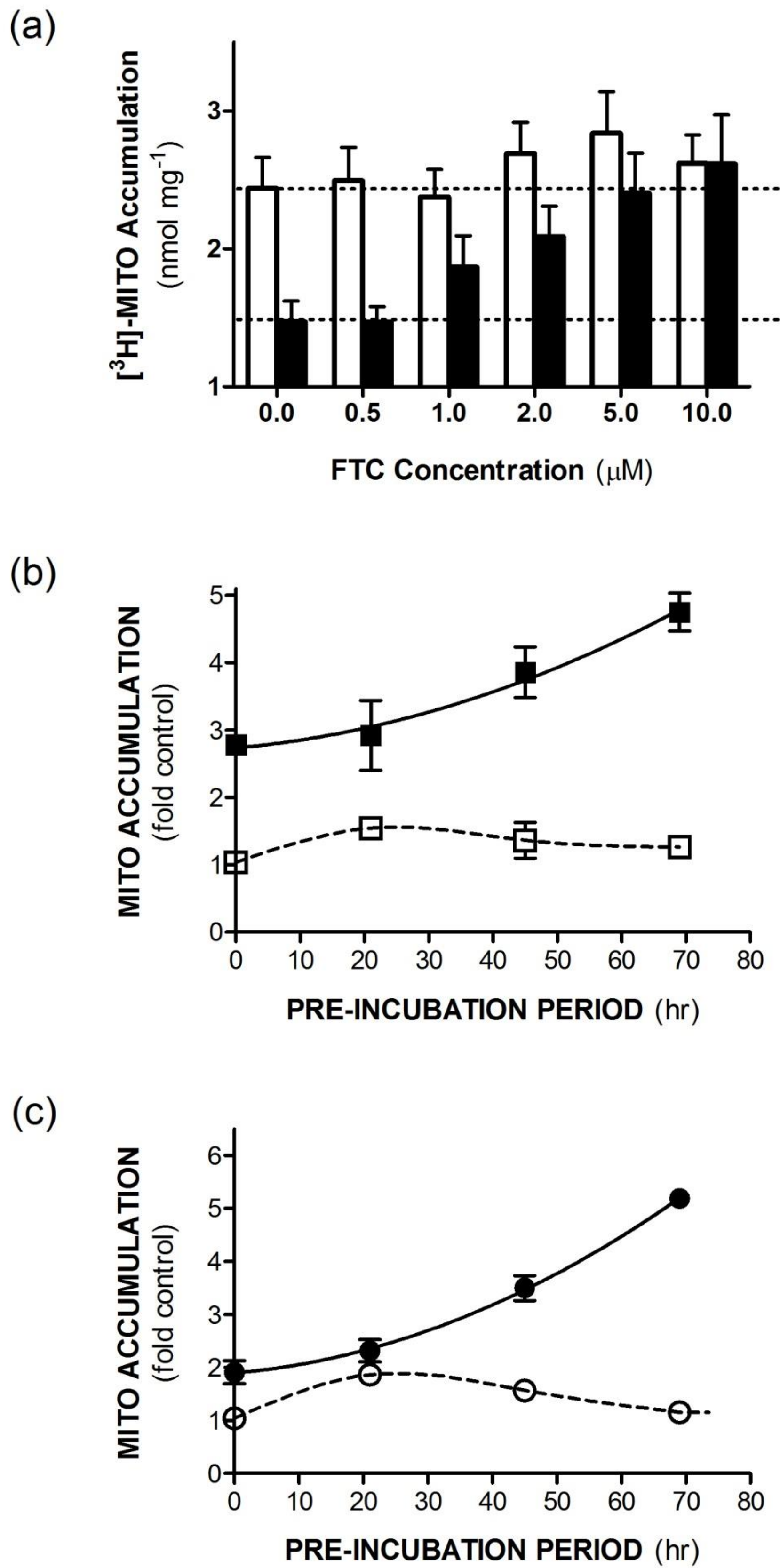

FIGURE 4

(a)

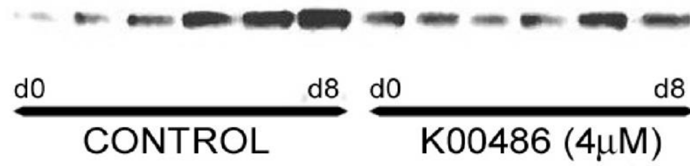

(b)

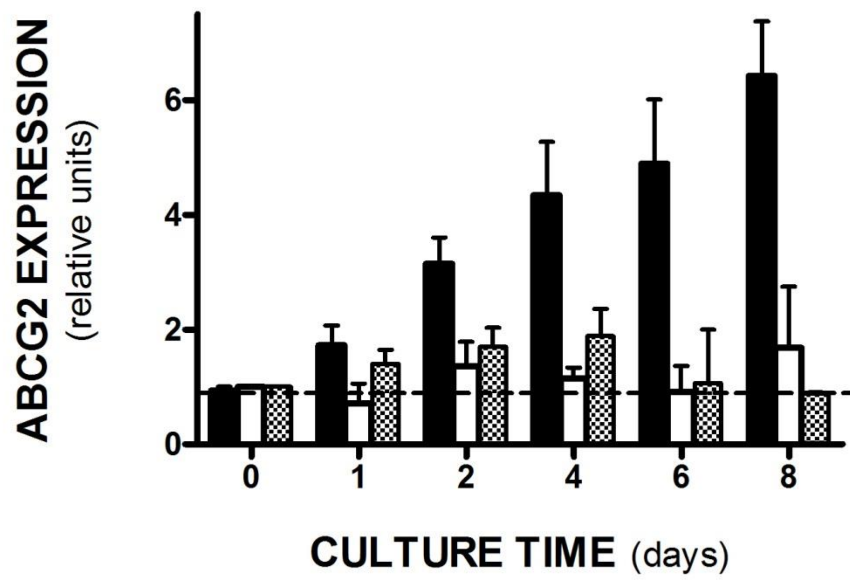

FIGURE 5